ELSEVIER

Journal of Nuclear Materials 270 (1999) 115–128

journal of nuclear materials

Role and significance of source hardening in radiation embrittlement of iron and ferritic steels

K. Linga Murty *

North Carolina State University, College of Engineering, Department of Nuclear Engineering, Box 7909, Raleigh, NC 27695-7909, USA

Received 29 April 1998; accepted 22 September 1998

Abstract

Radiation effects on ferritic steels used for pressure vessels and pure iron are investigated to examine the role of the source hardening term responsible for the yield point phenomena and dynamic strain-aging (DSA). The majority of the radiation hardening stems from friction hardening, and the source hardening term decreased with exposure to neutron radiation apparently due to the interaction of the interstitial impurities with radiation produced defects. This decrease in the source hardening suppressed DSA which in turn led to increased ductility with a simultaneous increase in the strength in the temperature range of DSA in the unirradiated condition. While the source hardening term was evaluated from an extrapolation of the work-hardening region to the elastic line for the ferritic steels, the grain-size variation of the yield strength in pure iron allowed a direct evaluation and demonstrated their equivalence. The influence of low-energy (Cd-cutoff) neutrons was studied by comparing radiation effects in specimens with and without Cd-wrapping. Inclusion of thermal neutrons along with fast resulted in a small decrease in the source hardening with a slight increase in the friction hardening which revealed a critical grain size below which exposure to total (fast and thermal) neutron spectrum resulted in a slight reduction in the yield stress compared to the exposure to only fast neutrons. This grain-size effect is shown to be in line with known radiation effects on friction and source hardening terms along with the observation that low-energy neutrons have a non-negligible effect on the mechanical properties of steels. In ferritic steels, however, despite their small grain size, exposure to total neutron spectrum yielded higher strengths than exposure to only fast neutrons. This behavior is consistent with the fact that the source hardening is small in these alloys and the radiation effect is due only to friction stress.

1. Introduction

Ferritic steels find many applications in fission reactors such as in the construction of pressure vessels in light water reactors, reactor support structures, steam generator housings in liquid metal fast breeder reactors, etc. Radiation embrittlement of the ferritic steels used for pressure boundary applications is usually monitored by Charpy impact tests on specimens fabricated from base, weld and heat-affected zone materials irradiated in surveillance programs in operating power reactors. This embrittlement is characterized in terms of decreased upper shelf energy accompanied by increased ductile to brittle transition temperature (DBTT). The extensive data base on various reactor vessel surveillance capsule programs revealed the influence of alloying elements such as Cu, Ni and P on the changes in DBTT and upper shelf energy along with the superimposed effects of radiation fluence and irradiation temperature [1,2].

Effects of alloying and impurity elements such as P, Cu, Ni, etc., have been well characterized, resulting in modern vessel materials and welding techniques with reduced amounts of these trace elements. In addition, the effects of interstitials such as C and N on the mechanical and fracture behaviors of these materials through strain aging have recently been shown to result in dips in the shelf energies and ductilities when plotted as a function of the test temperature [3,4]. While these factors were well established, the underlying micromechanisms responsible for these changes are at best

* Corresponding author. Tel.: +1-9 19 515 3657; fax: +1-9 19 515 5115.

0022-3115/99/$ – see front matter
PII: S0022-3115(98)00766-1

speculative and various attempts in the development of these mechanisms and models were hampered by the fact that the microscopic defects and defect complexes responsible for these effects are too small to be resolvable by standard electron microscopy techniques. Ultrafine defect characterization requires advanced techniques such as atom probe field ion microscopy, small angle neutron scattering, etc. Studies using positron annihilation spectroscopy [5] revealed that radiation-enhanced precipitation of carbides and nitrides plays a major role in radiation embrittlement of ferritic steels. These analyses imply that the elements such as Cu, Ni and P modify the kinetics of carbide precipitation thereby indirectly influencing radiation embrittlement. These observations are strikingly different from the currently believed premise based on the radiation enhanced precipitation of Cu [6]. In addition, interstitial impurities such as C and N lead to the well-known yield-point phenomena in ferritic steels which in turn exhibit serrated stress–strain curves or dynamic strain-aging (DSA). The DSA in turn results in a distinct drop in ductility, a phenomenon commonly referred to as *blue brittleness*. While there was the possibility of superimposed effects of radiation and blue-brittleness, it was clearly demonstrated that radiation suppresses DSA resulting in *improved ductility and fracture* characteristics in appropriate temperature and strain-rate regimes [7]. Moreover, materials irradiated in HFIR revealed sensitivity of radiation embrittlement on neutron flux spectrum. While it was thought in the past that only fast neutrons are responsible for changes in macroscopic properties of materials, these experimental investigations and recent computer simulations clearly showed that thermal and epithermal neutrons may make non-negligible contributions to the overall damage both in terms of microscopic defect production as well as the macroscopic property changes [8]. The additional embrittlement revealed in HFIR is now believed to be due to a large γ flux while thermal neutron effects seem to become noticeable only at very high thermal-to-fast flux ratios which, however, are not typical in commercial reactors.

A major factor influencing DSA and interstitial/solute interactions is the *source hardening* (Petch–unpinning coefficient) in Hall–Petch relation for the yield stress [9],

$$\sigma_y = \sigma_i + \sigma_s = \sigma_i + \frac{k_y}{\sqrt{D}}. \tag{1}$$

In this equation, σ_y is the yield stress, σ_i is the friction hardening, σ_s is the source hardening, k_y is the Hall–Petch coefficient and D is the grain size. It has been established that in ferritic steels, the source hardening decreases following radiation exposure [10]. The significance of the partitioning of the yield strength into friction and source hardening terms lies in the fact that the transition temperature from ductile to brittle fracture regimes may be evaluated using Cottrell brittle fracture theory [11]:

$$\Delta\mathrm{DBTT} = \frac{1 + \frac{2\Phi^2\sigma_y}{\sigma_i}\left(\frac{d\sigma_s}{d\Phi}\right)}{1 + \frac{\sigma_y}{\sigma_s}\left(\frac{\mathrm{d}\sigma_s}{\mathrm{dT}}\right)}\Delta\sigma_i,$$

$$\Delta\sigma_i = \alpha \mathrm{Gb}\sqrt{\phi t} = \alpha \mathrm{Gb}\sqrt{\Phi}. \tag{2}$$

In the above equation, DBTT is the ductile to brittle transition temperature, ϕ is neutron flux, Φ is fluence (ϕt), t is time of irradiation and T is test temperature. Thus, one needs to evaluate the influence of neutron irradiation and test temperature on both the friction and source hardening terms to characterize the change in DBTT. A rather thorough treatment of the significance of source hardening term in light of Eq. (2) has been presented by Olander [11]. However, lack of information on the fluence dependence of σ_s as well as other factors (temperature variation, etc.) makes it rather difficult to apply the above formulation for predicting the changes in radiation embrittlement of nuclear pressure vessels. Moreover, radiation embrittlement of ferritic steels is far more complex than using simple fracture theory. Nevertheless, these formulations based on basic theories of radiation hardening and fracture have substantial pedagogic advantages. Thus, the Nuclear Materials group at NCSU embarked on an extensive radiation effects program [12]. In order to obtain an understanding of the underlying micromechanisms, relatively pure Armco-iron and silicon-killed mild steel are used along with a number of low-alloy steels with varied compositions. We present here the experimental findings on Armco-Fe of varying grain sizes (50–300 μm) as well as some ferritic steels that are commonly used for reactor pressure vessels, demonstrating the role and significance of source hardening on the various phenomena. It has been demonstrated from studies on the yield point phenomena, in particular the serrations in DSA in various materials including mild steel [13], Armco-iron [14] as well as pressure vessel steels [15] that the degree of locking of the dislocations by interstitial impurity atoms decreases with exposure to neutron radiation leading to essentially a non-aging steel following exposure to high neutron fluences. This implies that source hardening decreases in irradiated steels. Since friction hardening increases with neutron fluence, these competing effects lead to interesting consequences when examined as a function of the grain size of the material [16].

2. Experimental details

As described in the introduction, while a number of alloys have been under investigation, we present here experimental work on silicon-killed mild steel, pure iron of varied grain sizes and some other steels. The chemical compositions of these materials are included in Table 1.

Table 1
Chemical composition of the steels and iron

	C	Mn	Si	S	P	Cu	Mo	Cr	Ni
Mid-steel [a]	0.05	0.39	0.001	0.012	–	0.091	–	0.0041	0.032
Armco-Fe [b]	0.01	0.04	0.02	0.01	0.01	–	–	–	–
1020	0.20	0.40	0.10	0.04	0.04	–	–	–	–
A516Gr70	0.20	0.98	0.02	0.02	0.02	0.24	0.03	0.20	0.16
A533B	0.25	1.38	–	0.02	0.01	0.13	0.61	–	0.61
A588	0.20	1.20	0.31	0.04	0.04	0.22	0.05	–	0.21

[a] wires – irradiated in HIFAR, Australia.
[b] grain sizes 50, 110, 190 and 300 μm.

Different grain sizes were obtained by appropriate thermo-mechanical treatments by the Defense Metallurgical Research Laboratory, India and mainly tensile specimens were machined due to a limitation in the amount of available material.

The samples (all but mild steel) were sealed in evacuated quartz tubes some of which were wrapped with Cd to screen out the low-energy neutrons whereas others were exposed to the total neutron spectrum. The prepared specimens were loaded in an aluminum canister as shown in Fig. 1 which indicates the matrix of specimens in the capsule C; the capsules A and B contained only Cd-wrapped specimens. Irradiation of the prepared specimens was performed in the PULSTAR reactor in the Department of Nuclear Engineering at North Carolina State University. Since the inherent structure of the PULSTAR core and reactivity considerations did not permit irradiation in the core, a vertical irradiation tube at core boundary was used as irradiation site. In addition, the vertical position of the jig in the canister was adjusted to the location of the maximum fast (>1 MeV) neutron flux of approximately 1.3×10^{12} n/cm^2 s at fullpower of 1 MW. High purity (99.9999%) Ni and Co wires were included for evaluating fast (>0.83 MeV) and total (>0.5 eV) flux. These measurements have not been made to-date using the flux monitors in the capsule C

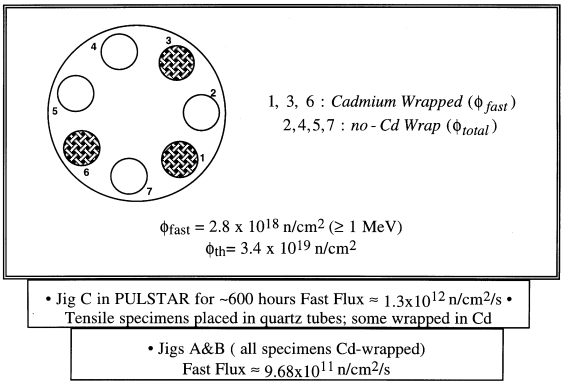

Fig. 1. Details of the materials and specimen types (Radiation Jig #C: inserted in PULSTAR).

but the fast flux has been evaluated from the measurements of the fast flux monitors in capsules A and B which yielded a value of 1.32×10^{12} n/cm^2 s for the fast flux [17] whereas the thermal flux is known to be about 12 times the fast flux. Irradiation temperature was the reactor operating temperature, about 323 K. The radiation jig C was left in the reactor for about 11 months with an effective full power time of 2.16×10^6 s. All the samples along with the aluminum canister became highly radioactive and thus were left in the reactor pool for more than one year for the activity to decay so that the samples can be handled without any remote handling facility. The fast and thermal neutron fluences were estimated to be about 2.8×10^{18} n/cm^2 and 3.4×10^{19} n/cm^2, respectively [18], while the fast fluence for the specimens in the A and B capsules was estimated to be about 6.5×10^{17} n/cm^2 [19]. The tensile tests were performed on a closed loop hydraulic Instron machine at a nominal strain rate of 9.6×10^{-5} s^{-1} with the load–elongation data collected using a MacIntosh computer. In some cases, 3-point bend tests were also performed using a compression jig which transforms a tensile load applied to its ends into a compressive load onto a v-notch specimen supported at three points. Load and load-line displacement signals were recorded on an x–y recorder and an Apple-II microcomputer. Area under the load–displacement curve up to the maximum load is taken to be a measure of the fracture initiation energy, E_1, while that after maximum load to fracture gives fracture propagation energy, E_2, so that the total energy is the sum of the two, $E_1 + E_2$.

Mild steel wires of 1 mm diameter and 38.5 mm gauge length were prepared from cold-drawn rimmed stock and were annealed in vacuo at 973 K resulting in a grain size of 0.038 mm. The annealed specimens were irradiated in high isotope flux Australian reactor (HIFAR), the heavy water moderated reactor at Lucas Heights, Australia. Different total neutron doses were obtained by insertion in the vertical holes; at positions close to the fuel plates for high doses and positions farther from the plates for lower doses. In all cases the time of irradiation was kept constant, and thus the different fluences were obtained by differing flux rates. Special precautions were taken to reduce γ-heating of

the specimens and the irradiation temperature is taken to be 353 K, the coolant temperature [13]. The wire specimens were tensile tested on a custom-made hard tensile machine at varied temperatures using appropriate salt baths under differing cross-head speeds. There is a possibility of post-irradiation-annealing at high temperatures, and thus the residence time is minimized except for waiting for thermal equilibrium to take place. As noted in the experimental results, no significant annealing of radiation damage occurred at temperatures below around 650 K for iron and steels, and around 500 K for mild steel. While multiple tests were performed on unirradiated samples, duplicate tests on irradiated materials were performed only at certain conditions due to the limited number of irradiated specimens. The following uncertainty maxima were noted: ±7.5 MPa for mild steel [13], ±9.5 MPa for Armco-iron [18] and ±11 MPa for other steels [19].

3. Results and discussion

3.1. Effect of neutron irradiation on friction and source hardening

As pointed out earlier, the yield or flow stress of metals can be regarded as comprised of the two components: the stress needed to unlock pinned dislocations and set them free into motion (source hardening, σ_s) and that experienced by the unlocked dislocations during their movement through the lattice (friction hardening, σ_i). The contribution of the source hardening is insignificant in fcc metals which manifests in smooth stress–strain curves (Fig. 2(a)). If these metals are irradiated the radiation produced defects pin the dislocation sources thereby resulting in a distinct yield point (Fig. 2(a)). The friction stress also increases due to the radiation produced defects which resist the dislocation motion. The situation in bcc metals (especially steels) will be more complex since the yield point already exists in the unirradiated condition due primarily to the locking of the dislocation sources by interstitial impurity atoms (IIAs) such as C and N. Following high radiation doses, *apparently* normal rounded yield is observed (Fig. 2(b)) which is taken to indicate little or no Luders propagation [20].

Since it is often difficult to obtain materials with different grain sizes particularly for commercial steels, an extrapolation technique by Makin–Minter [21] is used to evaluate the friction and source hardening components. Here, the work-hardening region of the stress–strain curve is extrapolated to lower strains and the intersection of the extrapolated curve with the elastic line (Fig. 3) gives the friction stress (σ_i) while the difference between the lower yield stress and friction stress gives the source hardening (σ_s). Armco-iron with different grain sizes helped to check the validity of this extrapolation technique. The yield strength was determined, following radiation exposure in PULSTAR to 6.5×10^{17} n/cm^2 (>1 MeV), as a function of the grain size from 50 μm to 300 μm, and the Hall–Petch plots for the unirradiated and irradiated iron are shown in Fig. 4. We note that the line corresponding to irradiated iron was shifted to higher stress (vertical axis) with a slight drop in the slope indicating increased friction stress with decreased source hardening. Table 2 summarizes the

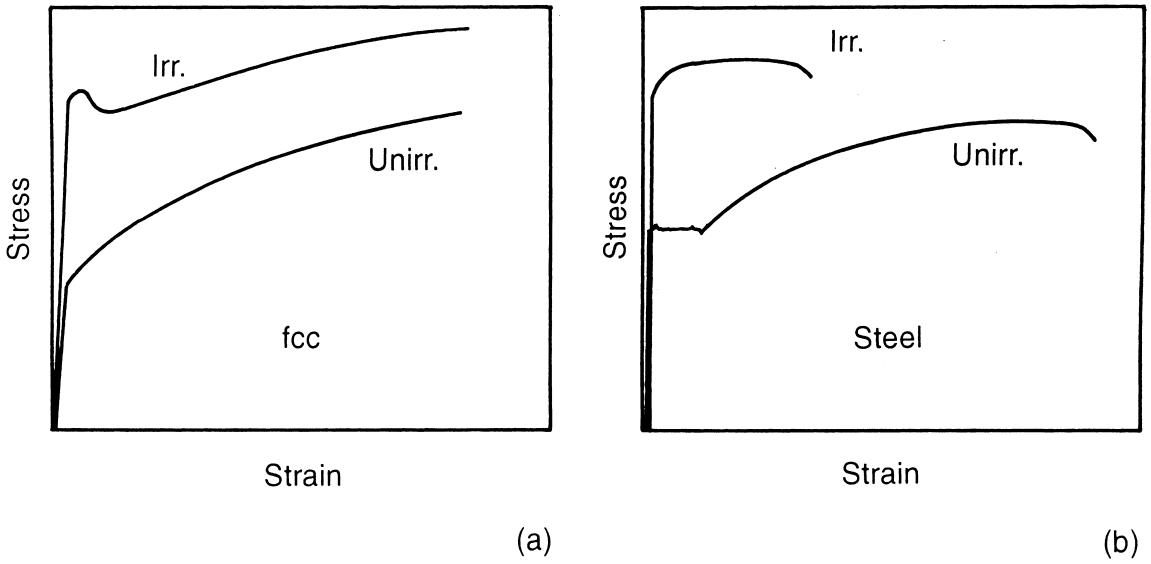

Fig. 2. Effect of radiation on σ–ε curves fcc (a) and bcc (b).

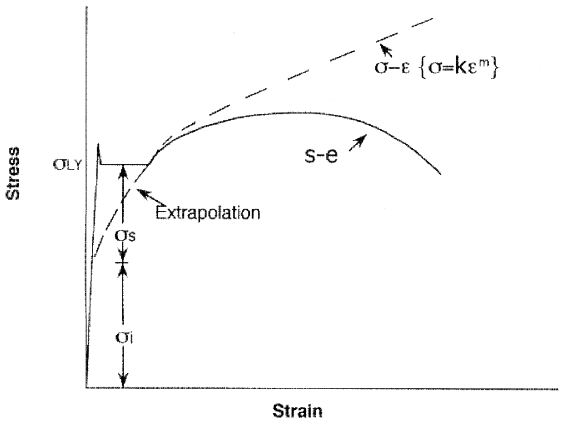

Fig. 3. Evaluation of σ_i and σ_s using extrapolation technique.

results. We note that the values of the unpinning coefficient (k_y) which defines the source hardening derived from these two techniques are essentially the same; this is seen to be valid before and after irradiation. The Hall–Petch coefficient (k_y) decreased from about 390 to 300 MPa $\sqrt{\mu m}$ following radiation exposure to 5×10^{17} n/cm^2.

Thus, the extrapolation technique was used to investigate the effect of test temperature on the friction and the source hardening components for Armco-iron with 50 μm grain size before and after irradiation (Fig. 5). In the unirradiated material σ_i decreased initially with increase in the test temperature reaching a minimum at maximum serrations in the stress–strain curve. Following radiation exposure, σ_i increased although at the highest test temperature of ≈650 K, annealing of radiation damage is apparent. Correspondingly, the source hardening term exhibited a maximum at the highest degree of locking or serrated yielding in the unirradiated material while it decreased

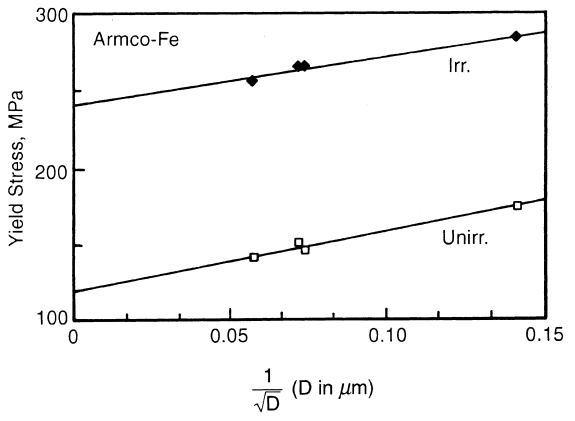

Fig. 4. Hall–Petch plot for unirradiated and irradiated Armco-Fe.

following radiation exposure reaching essentially a non-aging condition at temperatures around 500 K. We will return to this later following the description of the effect of the incremental neutron dose on these components.

3.2. Fluence dependence of yield stress

The effect of neutron fluence on the tensile characteristics was investigated on mild steel wires and Fig. 6 is a compilation of the stress–strain curves at ambient temperature. We note that the Luders strain increases with fluence (or flux) while essentially *rounded* yield with significant embrittlement is noted at the highest fast neutron (>1 MeV) fluence of 1.4×10^{19} n/cm^2. An increase in the lower yield stress due to radiation is observed to vary as one-third power of the fluence (Fig. 7),

$$\Delta\sigma = \sigma_{LY}^{irr} - \sigma_{LY}^{0} = 91.7(\phi t)^{1/3}, \tag{3}$$

where the stresses are in Pa and ϕt in n/cm^2. However, square-root dependence is predicted assuming that irradiation does not affect Petch-unpinning constant, k_y [20,22].

The friction and source hardening components were evaluated using the extrapolation technique and the derived friction stress did increase with square-root of the fluence (Fig. 8),

$$\sigma_i = 5.5 \times 10^7 + 0.11\sqrt{\phi t}, \tag{4}$$

where σ is in Pa and ϕt in n/cm^2. This is in agreement with the premise that the friction stress arises from long-range forces due to forest dislocations along with short-range interactions arising from vacancy– and interstitial–solute complexes produced in irradiated steels:

$$\sigma_i = \alpha G b\sqrt{\rho} + \beta\sqrt{N}, \tag{5}$$

where G is the shear modulus, b Burgers vector, ρ the dislocation density, N the volumetric density of planar obstacles, α a numerical constant (∼1) and β a material constant (the exact expression for β depends on the specific obstacles such as depleted zones, second phase particles, etc). Assuming that ρ and N increase linearly with fluence, one obtains the square-root dependence as noted above. The source hardening, however, decreased with neutron fluence as noted Fig. 8. This is the reason for the decreased exponent (1/3) exhibited by the yield stress.

The yield point phenomena in steels are primarily due to the locking of the dislocations by interstitial C and N, and there is both indirect and direct evidence showing the decrease of the concentration of free C and N (i.e. in solution) following neutron irradiation. Dynamic strain-aging studies by Murty and Hall [23] on irradiated mild steel indicated that with increase in fluence, the degree of locking of the dislocations by interstitial impurities decreased, the critical temperature for the onset of serra-

Table 2
Stress components derived from extrapolation technique and grain-size variation

	Extrapolation technique*			Hall–Petch relation		
Armco-Fe	σ_y, MPa	σ_i, MPa	σ_s, MPa	σ_i, MPa	k_y, MPa$\sqrt{\mu m}$	σ_s, [a] MPa
Unirradiated	174 ± 9	119 ± 6	55 ± 6	118.4 ± 4.6	396.1 ± 49	56.0 ± 6.9
irradiated	275 ± 9	233 ± 6	42 ± 6	240.7 ± 4.8	305.7 ± 51	43.2 ± 7.2

[a] 50 μm grain size.

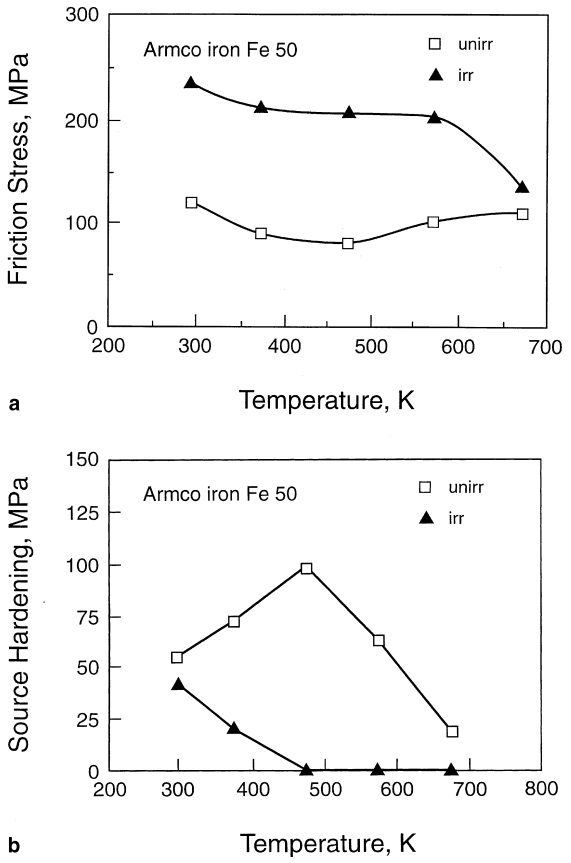

Fig. 5. Effect of neutron irradiation on temperature variation of friction hardening (a) and source hardening (b) in Armco-iron.

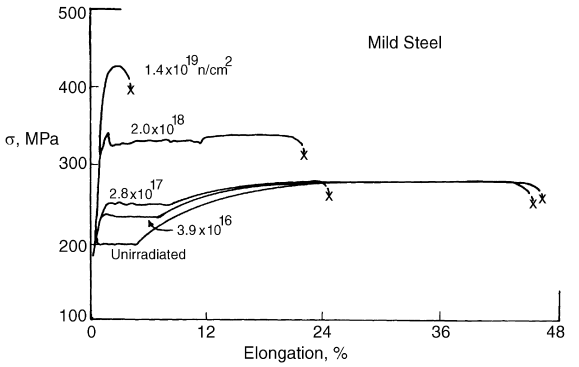

Fig. 6. Effect of neutron irradiation on tensile σ–ε curves for mild steel at 300 K.

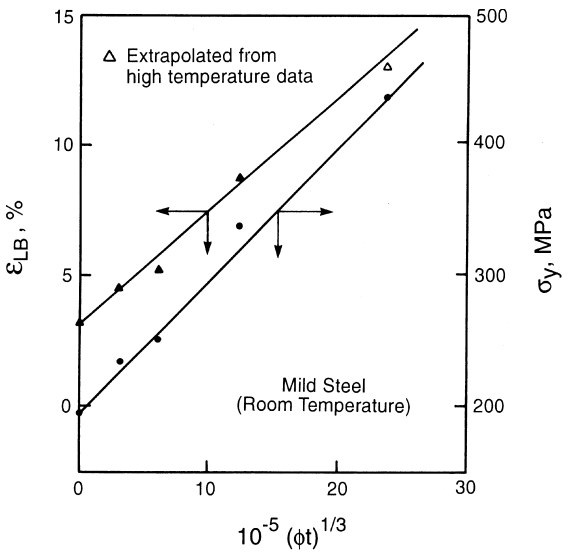

Fig. 7. Effect of radiation fluence on yield stress (σ_y) and Luders strain (ε_{LB}).

tions increased and temperature range of DSA lowered, ultimately resulting in non-aging steel at fast (>1 MeV) neutron fluence in excess of 10^{18} n/cm^2. Murty and Mahmood [24] reported that partially denitrided steel exhibited DSA very similar to irradiated steel thereby giving further evidence as to the decreased amounts of IIAs in solution following radiation. Murty [25] examined the effect of incremental neutron dose on static strain-aging kinetics and demonstrated that the aging kinetics are slowed and irradiation fluences greater than 10^{18} n/cm^2 rendered the steel non-aging. These results imply that IIAs combine with radiation induced point defects such as vacancies and interstitials, either individual defects or loops, to form complexes. These complexes are probably responsible for part of the increase in friction hardening. At the same time, the creation of these complexes results in reduced amounts of IIAs in solution available for locking the dislocation sources. McLennan and Hall [26] indeed found from internal friction experiments that the concentration of C

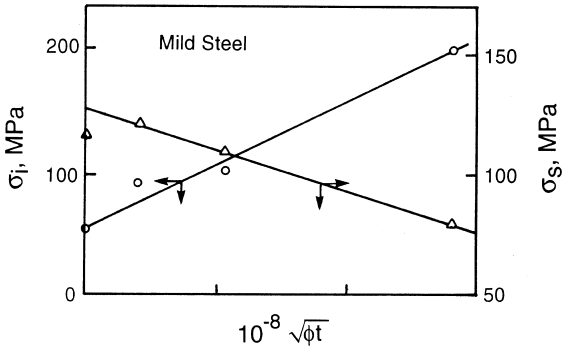

Fig. 8. Influence of neutron fluence on friction and source hardening components of the yield stress.

in solution decreased by a factor of 4 in steels after irradiation to about 10^{19} n/cm^2.

It is known in steels, that the Luders strain varies linearly with the yield stress and thus the Luders strain also increases linearly with cube root of fluence as per the yield stress (Fig. 7). Temperature dependence of Luders strain at the highest fluence of 1.4×10^{19} n/cm^2 revealed that distinct Luders bands appeared at temperatures greater than ~448 K and extrapolation of the high temperature results to room temperature indicated a value of ~13% in agreement with data in Fig. 7. Thus at the highest fluence, the specimen exhibited severe localized deformation and failed during Luders band propagation itself before reaching the strain hardening region. The increase in Luders strain along with the corresponding decrease in source hardening in irradiated steels implies that the rate of work-hardening should decrease as neutron dose increases. Indeed, the work-hardening exponent decreased from ~0.34 for the unirradiated steel to ~0.19 at a neutron fluence of 2×10^{18} n/cm^2.

3.3. Synergistic effects of IIAs and radiation-produced defects

The fact that radiation exposure results in reduced IIAs in solution leads to reduced *blue brittleness* while radiation hardening and embrittlement also accompany. The question arises as to the competing effects of blue brittleness or DSA and neutron irradiation on the ductility, and at appropriate strain-rates and temperatures suppression of DSA should lead to increased ductility along with increased strength. Fig. 9 compiles the tensile curves at 373 K as a function of neutron irradiation and illustrates these synergistic effects [27]. While *normal* radiation hardening and embrittlement are noted at ambient (Fig. 6), the pronounced embrittlement noted at 373 K due to DSA [just at the start of serrations] in the unirradiated material is completely suppressed following radiation exposure to 2×10^{18} n/cm^2 and the ductility increased from 11% before irradiation to 20% following exposure to 4×10^{16} n/cm^2, to 19% at 3×10^{17} n/cm^2 and to 22% at 2×10^{18} n/cm^2; these *increases* in the ductility are accompanied by radiation hardening. At the highest fluence used here, however, the ductility decreased to about 2% along with pronounced increase in the strength as normally observed. These results at the intermediate fluences translate to the fact that exposure to high energy neutrons should lead to *improved* toughness due to the suppression of DSA. The toughness defined as the energy to fracture is evaluated from the areas under the true σ–ε curves and the effect of neutron irradiation to 2×10^{18} n/cm^2 is illustrated in Fig. 10 where the toughness (J) is plotted versus test temperature. We note normal embrittlement at ambient temperature while increased toughness values are observed at elevated temperatures following radiation exposure. Further increase at temperatures higher than 500 K is believed to arise from post-irradiation-annealing.

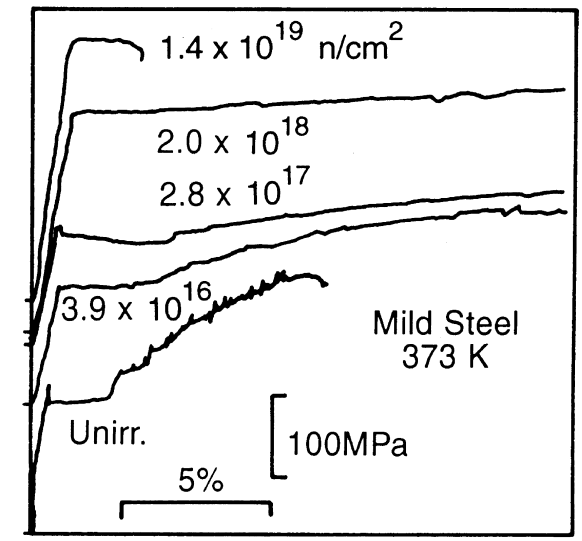

Fig. 9. Effect of neutron irradiation on tensile σ–ε curves for mild steel at 373 K.

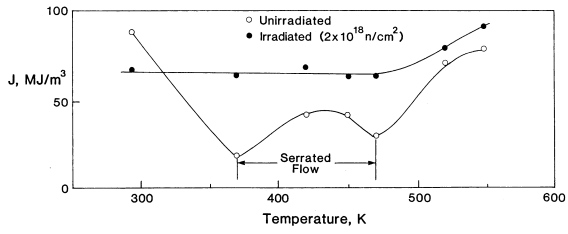

Fig. 10. Effect of DSA and neutron irradiation on the temperature dependence of energy to fracture.

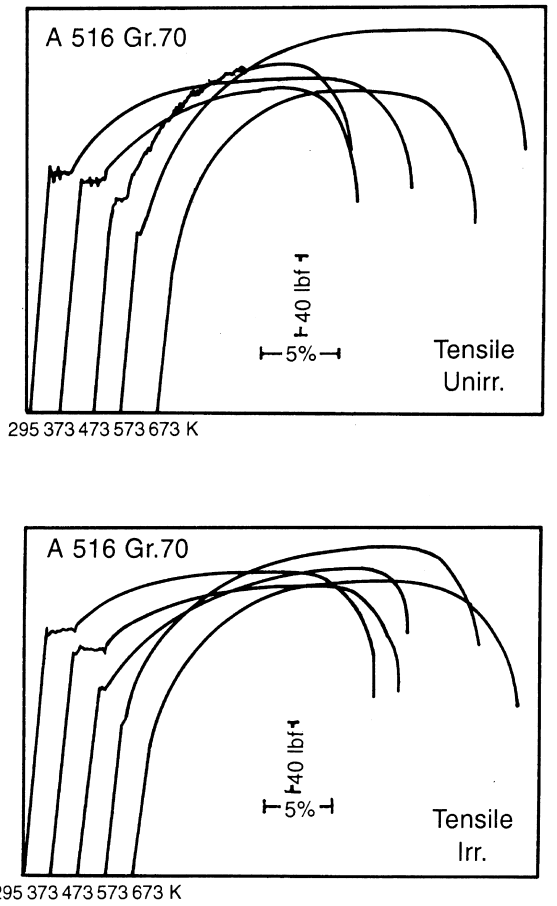

Fig. 11. Load-elongation curves for A516Gr70 steel in the unirradiated (a) and irradiated (b) conditions.

3.4. A516Gr70 and A533B steels

The mechanical properties of A516Gr70 steel are examined in the light of friction and source hardening analysis described earlier, and Fig. 11 is a compilation of the load-elongation curves at different test temperatures from ambient to 673 K in both the unirradiated (Fig. 11(a)) and following irradiation to 2×10^{18} n/cm^2 (Fig. 11(b)). These curves clearly depict the dynamic strain-aging effect with serrations at 473 K for the unirradiated condition whereas following radiation exposure such serrations are not as clearly discernible except for slight load-fluctuations at 573 K. The DSA effect in these steels is very small compared to that noted earlier in the silicon-killed mild steel (Figs. 6 and 9) and is similar to the observations in A533B steel [3]. The effect of neutron irradiation on the temperature dependence of the yield stress is depicted in Fig. 12(a) while similar data on the total elongation are shown in Fig. 12(b). Normal radiation hardening is noted at temperatures below 473 K (Fig. 12(a)), the temperature corresponding to DSA in unirradiated condition. At higher temperatures, either no effect or some softening is noted which could be due both to the absence of DSA following irradiation and some annealing of radiation damage. This is more clearly depicted in the temperature variation of the ductility (Fig. 12(b)) where we note embrittlement at ambient while increased ductility following radiation exposure at 373 and 473 K where DSA is observed in the unirradiated material. This improvement in ductility is due to the suppression of DSA as seen earlier; again, decreased ductility is noted at 573 K, as expected, following radiation exposure. At the highest temperature of 673 K, essentially no change is noted due perhaps to the annealing of the radiation damage.

The stress–strain curves depicted in Fig. 11(a) and (b) were used to evaluate the two stress components by the extrapolation technique. Fig. 13(a) and (b) show the effect of neutron irradiation on the friction and source hardening terms and we note an increase in the friction component (Fig. 13(a)) only at temperatures below the DSA range ($\leqslant$ 473 K) and little effect is noted at higher temperatures. Fig. 13(b) depicts the temperature dependence of the source hardening and a decrease is seen at all temperatures. This implies that neutron irradiation

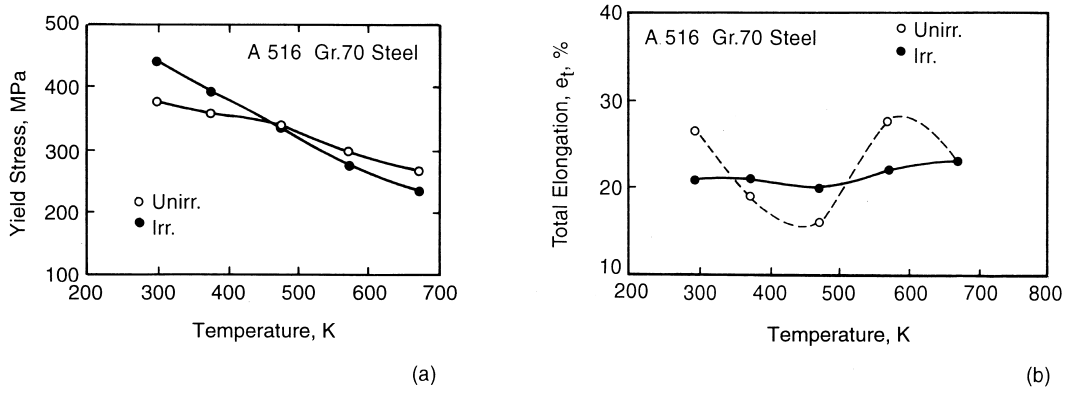

Fig. 12. Effect of neutron radiation on the temperature variation of yield stress (a) and ductility (b) in A516Gr70 steel.

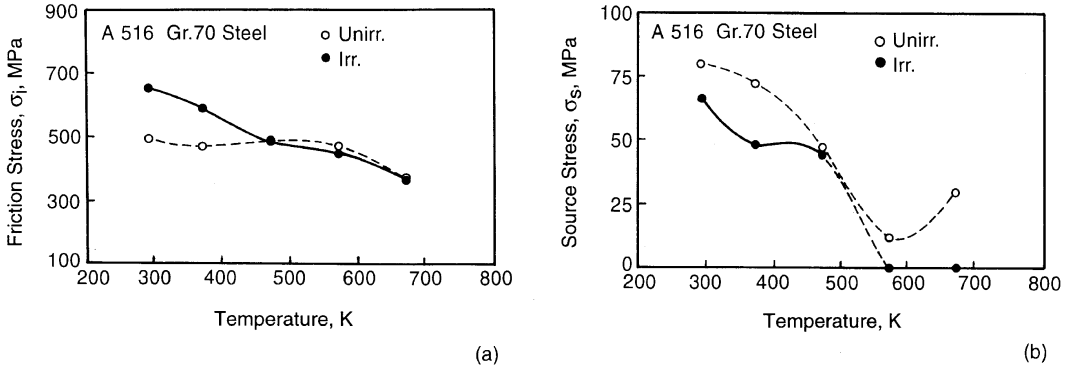

Fig. 13. Effect of neutron irradiation on the temperature variation of friction (a) and source (b) hardening terms in A516Gr70 steel.

results in decreased concentrations of IIAs in solution as pointed out earlier.

Load versus displacement curves for 3-point bend tests in the unirradiated and irradiated conditions revealed no serrations due to DSA, although these effects are noted in the temperature variation of the energy to fracture. As shown in Fig. 14, the fracture energy exhibits a dip between 400 and 650 K which is the temperature range of DSA. It is to be noted that this temperature range corresponds to the upper shelf regime where temperature independent fracture energy is observed in Charpy tests. Because of the high strain-rates in the Charpy tests, the effect of DSA is not discernible. The effect of neutron radiation is a decrease in the fracture energy as noted at temperatures below about 400 K whereas the energy values were higher at 473 and 573 K, where the unirradiated material exhibits DSA. It is to be noted that the irradiated material does exhibit a dip (albeit small) with the energy minimum at slightly higher temperature indicating again the decreased amount of IIAs in solution.

We also examined the tensile characteristics of A533B steel taken from the HSST04 plate at one-fourth thickness and the energy to fracture was evaluated using 3-point bend specimens of Charpy geometry. In addition, elastic–plastic fracture toughness [J_{IC}] has been determined on these Charpy size precracked samples using unloading compliance technique [28]. The tensile test results are very similar to those on A516Gr70 steel and these results may be found elsewhere [29]. Fig. 15 depicts the energy to fracture as evaluated from the areas under the load–displacement curves in the 3-point bend tests for two different loading rates as a function of the test temperature. As before, although the range of temperatures corresponds to the upper shelf where usually constant energy is noted [in the Charpy tests], distinct dips in toughness are observed in the DSA regions. The critical temperature at which the energy minima occur increases with increased rate of deformation with an activation energy of 118 kJ/mole that lies between those for the appearance and disappearance of serrations in the tensile tests. An extrapolation of these data to the high deformation rates corresponding to the Charpy tests reveals that these minima should occur at very high temperatures; thus, these effects were not discernible in the Charpy tests.

The effect of neutron irradiation has been examined on the elastic–plastic crack initiation fracture toughness.

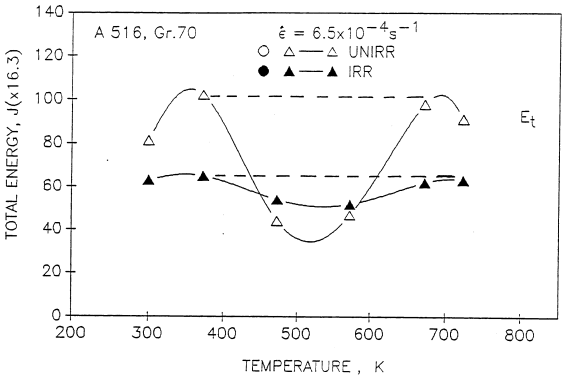

Fig. 14. Effect of neutron irradiation on temperature variation of fracture energy in A516Gr70 steel.

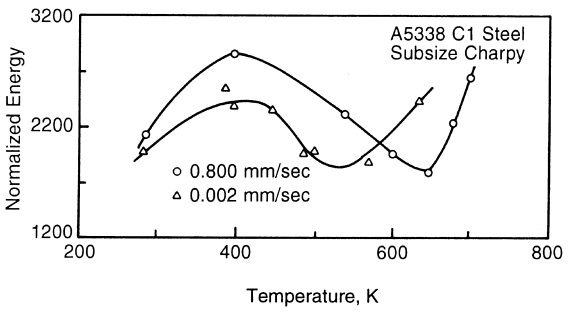

Fig. 15. Effect of DSA on temperature variation of fracture energy (A533B steel).

J_q (in place of J_{IC} since the validity criteria for testing were not satisfied), following fast neutron exposure at the reactor operating temperature of 50°C. Fig. 16 summarizes the temperature dependence of the fracture toughness for the unirradiated and irradiated materials which illustrates the characteristic dips. Moreover, the temperature for toughness minimum increased following neutron irradiation again illustrating the fact that neutron radiation results in *reduced* amounts of IIAs *in solution*. Although the differences are relatively small considering the experimental errors, radiation embrittlement *is* observed at high temperatures while improvement in the toughness is noted at temperatures below the energy minima. It is to be pointed out that radiation *does not* eliminate DSA but *postpones* it to higher temperatures. The synergistic effects of radiation produced defects and IIAs are sensitive to the composition of the steels.

3.5. Armco-Fe versus mild steels

As we have seen in the preceding sections, the occurrence of DSA causes increases in the tensile strength and strain hardening exponent with an accompanying loss in ductility. The increased strain hardening exponent is expected to result in an increased crack initiation ductile fracture toughness [30] since according to Hahn and Rosenfield [31],

$$r_p = n^2, \tag{6}$$

where r_p is the plastic zone size in inches. This relation has been shown to be valid in many metals and Srinivas et al. [30] have demonstrated the correlation in Armco-iron. It is also pointed out [14] that as long as the stress state is not changing, the void growth is decelerated directly with the strain hardening exponent. In contrast, we have seen above that DSA results in decreased energy to fracture in mild steels. As noted in Fig. 16, the fracture toughness of A533B class 1 steel, represented in terms of J_q, decreases markedly with increasing temperature in the DSA regime and attains a minimum value at 523 K. These results are reproduced in Fig. 17(a) and (b) for Armco-iron and A533B steel respectively along with fracture morphologies in the DSA regimes.

Thus, an increase in n leads to larger plastic zone and decelerated void growth rate in both cases. Void nucleation in Armco-iron, a particle-free system, seems to occur by slip band intersection [14,30] and thus, a relatively higher strain is required to nucleate the voids, which implies a greater energy input. This feature therefore combines with the influence of n in suppressing the void growth rate to give rise to enhanced J_{IC} in the DSA regime in iron as seen in Fig. 17(a). In contrast, in particle bearing systems such as A533B steel (microstructure of ferrite and bainite with carbide particles), void nucleation should occur at second phase particles either by decohesion of the particle–matrix interface or by the breaking of the particles. The occurrence of DSA leads to increased flow stress along with the strain hardening coefficient which enable the attainment of the critical stress for interface decohesion at relatively lower

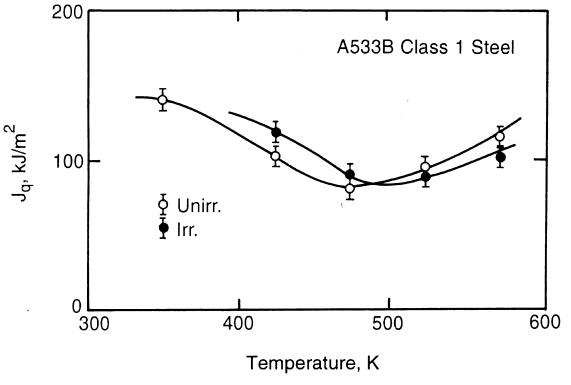

Fig. 16. Effect of neutron irradiation on temperature dependence of fracture toughness (J_q) for A533B steel.

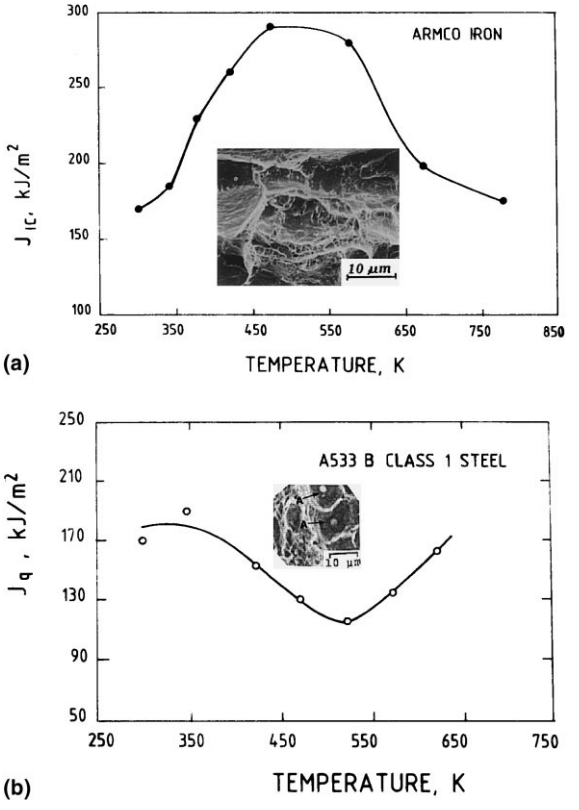

Fig. 17. Variation of fracture toughness for Armco-iron (a) and A533B steel (b) along with SEM fractographs at DSA.

strains [14]. Further, in the particle bearing systems the close spacing between adjacent particles restricts the extent of void growth in which case the fracture strain (comprising nucleation and growth strains) is dominated by the nucleation strain thereby lowering the J_{IC} in the DSA regime. The role of particles in the fracture process of A533B steel is evident from the fractograph shown in Fig. 17(b) where dimples are seen to be associated with the particles at 523 K corresponding to the minimum in fracture toughness.

3.6. Effect of fast versus total flux

As pointed out in the section on experimental aspects, irradiation studies were made on iron of varied grain sizes and some ferritic steels to examine the influence of low-energy (Cd-cutoff) neutrons on the tensile characteristics by using samples with and without cadmium wrapping. Fig. 18 compiles room-temperature load–elongation curves for Armco-iron of small (50 μm) and large (300 μm) grain sizes and for 1020 and A588 steels obtained on samples taken from the capsule C with and without cadmium wrapping. Cadmium wrapped materials correspond to fast neutron exposures while without wrapping implies total neutron spectrum which includes fast and thermal (i.e., below the Cd-cutoff). The steel samples reveal that the exposures which include low-energy ($\leqslant 0.5$ eV) neutrons resulted in increased strengthening accompanied by increased ductility implying the *non-negligible* effect of low-energy neutrons on radiation hardening phenomena. The changes in strength are small, due to relatively low-fluence levels, but discernible within experimental error.

Large grained iron samples showed no discernible difference between the fast and total spectra whereas at small grain sizes, increased hardening and decreased ductility were observed following exposure to *only* fast neutrons (i.e., cadmium wrapped) compared to the specimens exposed to the neutrons with all energies. For the smallest grain size used here, namely 50 μm, duplicate tests were performed and the Cd-wrapped (exposed to only fast neutrons) exhibited an yield stress of 305 ± 7 MPa compared to 285 ± 6 MPa obtained when exposed to total neutron spectrum. At intermediate grain sizes a gradual change, albeit small, is noted while A516 steel exhibited essentially the same effect as 1020 and A588 steels. Fig. 19 is a bar chart depicting the yield strengths of the various steels and Armco-iron of different grain sizes following exposure to fast and total neutrons, and the maximum possible errors are indicated. We note that as grain size decreases from 190 to 50 μm, exposure to low-energy neutrons along with fast neutrons resulted in

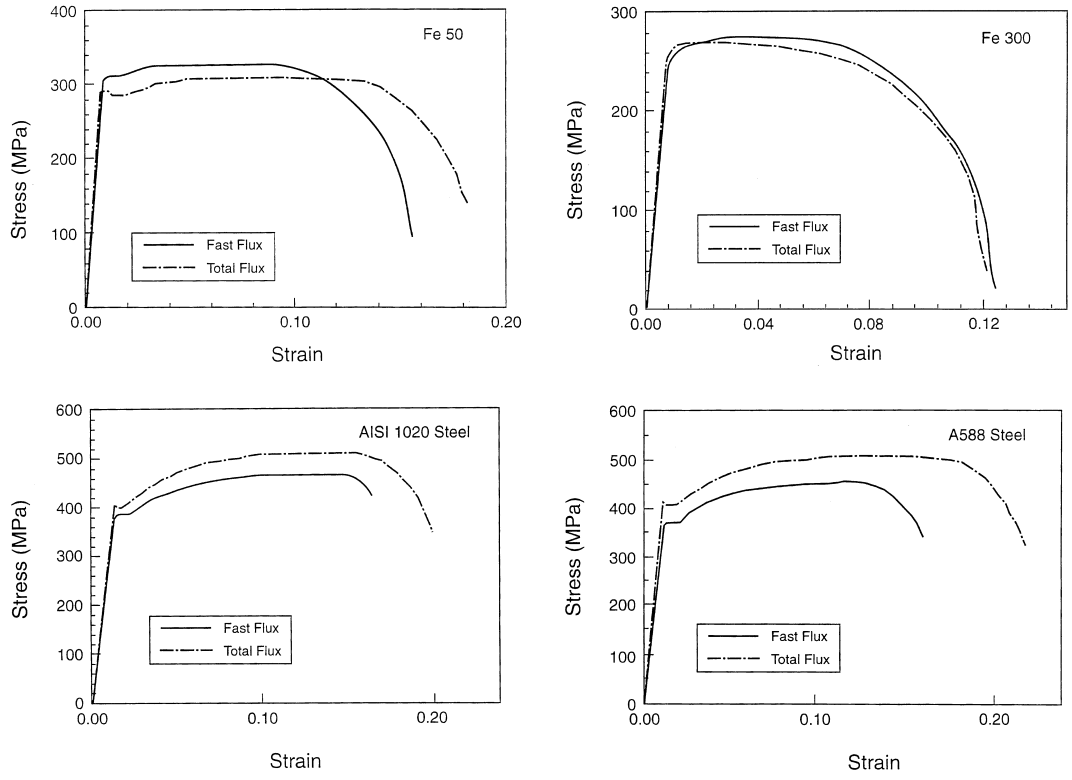

Fig. 18. Effect of fast (Cd-wrapped) and total neutron energy spectra on load-elongation curves.

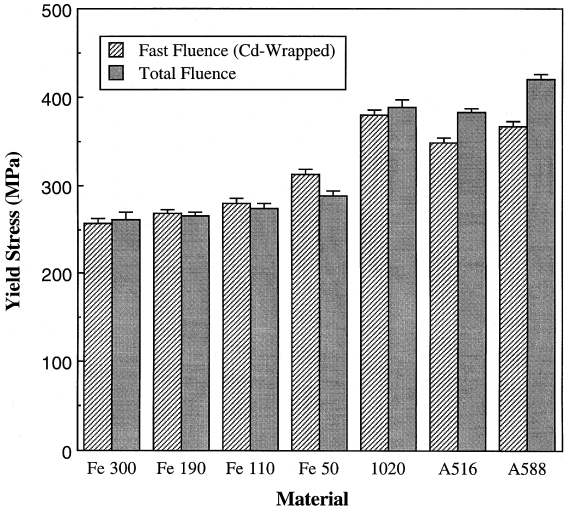

Fig. 19. Bar chart of yield stresses for Armco-iron and various steels following fast and total neutron radiation exposure.

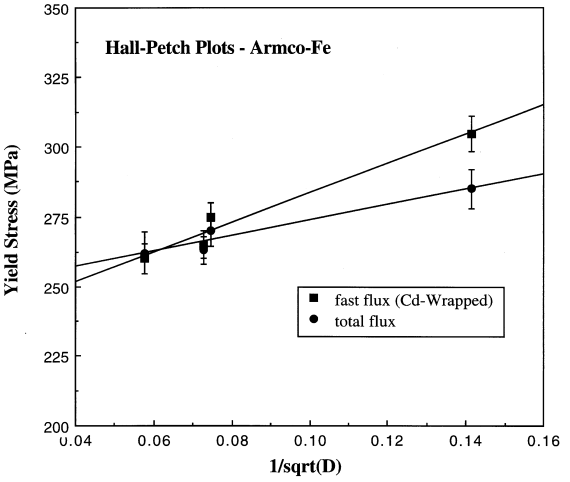

Fig. 20. Effects of fast and total neutron fluences on Hall–Petch plots for Armco-iron.

lower radiation hardening whereas all three steels showed that the total neutron exposure resulted in increased hardening compared to only fast neutrons.

We attempt first to explain the grain-size effect noted in Armco-iron by examining the influence of radiation exposure on the friction and source hardening terms. It is convenient to evaluate these effects by making Hall–Petch plots as in Fig. 20 where we plotted the yield stress as a function of $D^{-0.5}$ following radiation exposure to total and fast neutrons. As noted before, we expect the friction hardening to increase and source hardening to decrease due to irradiation which means that the line in Fig. 20 gets displaced to higher values along the y-axis (stress) with a decrease in the slope (unpinning constant k_y and source hardening σ_s). Although absolute values of the stresses do not show distinct differences at large grain sizes, the Hall–Petch plots clearly delineate the effects of fast vs. total neutron irradiation.

Ferritic steels commonly used in pressure boundary and reactor support applications have very small grain sizes, typically $\leqslant 50$ μm. But radiation hardening in these materials is opposite to what has been noted in Armco-Fe of small grain sizes. A plausible explanation for this observation lies in the fact that the source hardening and the Petch coefficient (k_y) are very small in these steels to start with which is easily noted from the fact that the yield points are not very distinct and also the serration height during dynamic strain aging at appropriate strain-rates and temperatures is relatively small. This implies that the slope of the Hall–Petch line is very small in the unirradiated condition as depicted in the schematic representation of the grain-size effect in these steels (Fig. 21); data on grain-size effect of these steels are not available to-date. Once these materials are exposed to fast neutrons, the hardening will all be due primarily to the friction stress with essentially negligible source hardening thereby resulting in a grain-size independent yield stress (horizontal line in Hall–Petch plot, Fig. 21). Exposure to low-energy neutrons along with fast neutrons is expected to result in a slight increase in the friction hardening only, thereby resulting in a Hall–Petch line parallel to that noted following exposure to only fast neutrons. Thus, exposure to the total neutron energy spectrum in these steels will lead to an additional hardening compared to only fast neutrons *irrespective of the grain size*. The partitioning of the yield stress into friction and source hardening terms thus lends explanation and support to the present experimental observations in both

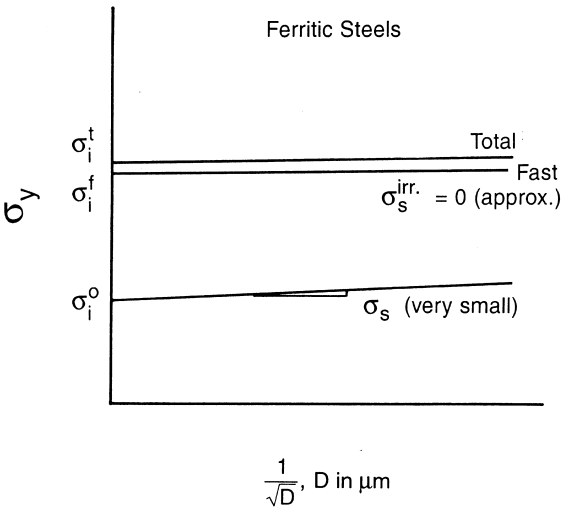

Fig. 21. Effects of fast and total neutron fluences on Hall–Petch plots (schematic) for ferritic steels.

Armco-Fe and ferritic steels. Further work to higher fluences and larger range of grain sizes (for iron) would confirm these findings and explanations.

4. Summary

The influence of neutron irradiation on the friction and source hardening terms comprising the yield stress was investigated in Armco-Fe, mild steel and several commonly used nuclear reactor pressure vessel steels. While the source hardening term was evaluated from an extrapolation of the work-hardening region to elastic line for the ferritic steels, the grain size variation of the yield strength in pure iron allowed a direct evaluation and demonstrated their equivalence. The friction hardening increased with square-root of fluence while source hardening decreased, resulting in the cube-root variation of the yield stress. The decreased source hardening in the irradiated material lead to synergistic effect of IIAs and radiation produced defects which in turn suppressed *blue brittleness* resulting in *increased* ductility along with radiation hardening in the strain-rate and temperature regimes of DSA in unirradiated material. These synergistic effects are shown to result in apparent *improvements* in energy to fracture as well as in J_{IC} in the DSA region of unirradiated steels while normal radiation embrittlement is noted at low and high temperatures. It was shown that radiation postpones the onset of DSA to higher temperatures.

The influence of low-energy (Cd-cutoff) neutrons was studied by comparing radiation effects in specimen with and without Cd-wrapping. Inclusion of thermal neutrons along with fast resulted in further decrease in the source hardening with a slight increase in the friction hardening which revealed a critical grain size below which exposure to total (fast and thermal) neutron spectrum resulted in a slight reduction in the yield stress compared to the exposure to only fast neutrons. This grain-size effect is shown to be in line with known radiation effects on friction and source hardening terms along with the observation that low energy neutrons have a *nonnegligible* effect on the mechanical properties of steels. In ferritic steels, however, despite their small grain size, exposure to total neutron spectrum yielded higher strengths than exposure to only fast neutrons. This behavior is consistent with the fact that the source hardening is small in these alloys and radiation effect is due only to friction stress.

Acknowledgements

I would like to express my sincere appreciation to Professor E.O. Hall, formerly at the University of Newcastle, Australia, who introduced me to this subject of yield point phenomena in steels and radiation effects on them. Contributions from many of my former students at NC State are gratefully acknowledged. I have been immensely benefited, in this research, through teaching the course on *Nuclear Materials* at NC State since 1981, in particular by using the book, *Fundamental Aspects of Nuclear Reactor Fuel Elements*, by Professor Olander which formed the basis for many of the analyses used here.

References

[1] G.E. Lucas, G.R. Odette, E. Mader, F. Haggag, R. Nanstad, Effects of composition and temperature on irradiation hardening of pressure vessel steels, Proceedings of the Fifth International Symposium on Environmental Degradation of Materials in Nuclear Power Systems – Water Reactors, American Nuclear Society, 1992, pp. 696–703.
[2] M.S. Wechsler, K.L. Murty, Proceedings of Symposium on Irradiation–Enhanced Materials Science and Engineering, Metall. Trans. 20A (1989) 2637.
[3] Y.H. Jung, K.L. Murty, Effect of interstitial impurities on fracture characteristics of A533B class1 pressure vessel steel, 13th International Symposium on Influence of Radiation on Mechanical Properties, ASTM STP 956, 1987, pp. 395–407.
[4] J.H. Hong, K.L. Murty, Effect of dynamic strain aging and neutron irradiation on fracture characteristics of various steels and iron, Proceedings of ASM Symposium on Microstructure and Mechanical Properties of Aging Materials, Chicago, 26–29 October 1992, pp. 391–397.
[5] G. Brauer, L. Liszkay, B. Molnar, R. Krause, Nucl. Eng. Design 127 (1991) 47.
[6] G.R. Odette, Scripta Met. 17 (1983) 1183; G.R. Odette, Radiation induced microstructural evolution in reactor pressure vessel steels, Proceedings of Mater. Res. Soc. Symp. 373 (1995) 137.
[7] K.L. Murty, Nature 308 (1984) 51.
[8] K. Farrell, S.T. Mahmood, R.E. Stoller, L.K. Mansur, J. Nucl. Mater. 210 (1994) 268.
[9] G.E. Dieter, Mechanical Metallurgy, 3rd ed., McGraw-Hill, New York, 1986, p. 199.
[10] K.L. Murty, D.J. Oh, Scripta Met. 17 (1983) 317–320.
[11] D.R. Olander, Fundamental aspects of nuclear reactor fuel elements, energy research and development administration, Document #TID-26711-P1, 1976, p. 418.
[12] K.L. Murty, J. Met. Sept. (1986) 28.
[13] K.L. Murty, E.O. Hall, Dynamic strain aging and neutron irradiation in mild steel, ASTM STP 611 (1976) 53–71.
[14] M. Srinivas, G. Malakondaiah, K. Linga Murty, P. Rama Rao, Scripta Met. 25 (1991) 2585.
[15] S.T. Mahmood, K. Al-Otaibi, Y.H. Jung, K.L. Murty, J. Test Eval. 18 (1990) 332.
[16] S.B. Kass, K.L. Murty, Effect of neutron irradiation on mechanical properties of ferritic steels, in: P.K. Liaw et al., (Eds.), Proceedings of Second International Conference on Microstructures and Mechanical Properties of Aging Materials, TMS, 1996, p. 27.

[17] J. Hong, R. Zou, J. Britt, K.L. Murty, Role of friction and source hardening in DSA and radiation embrittlement of ferritic steels and iron, Proceedings of SMiRT-12, paper F09/3, 1993.
[18] S.L. Kass, Dynamic strain aging and radiation embrittlement in mild steels and Armco iron, M.N.E. Report, N.C. State University, Raleigh, NC, 1994.
[19] Y. Zou, Dynamic Strain Aging and Fast Neutron Irradiation Effects in Ferritic A516Gr.70 Steel and Armco Iron, MS thesis, N.C. State University, Raleigh NC (1993).
[20] E.O. Hall, Yield Point Phenomena in Metals and Alloys, Macmillan, London, 1970.
[21] M.J. Makin, F.J. Minter, Acta Metall. 8 (1960) 691.
[22] R.W. Nichols, D.R. Harries, Radiation Effects on Metals and Neutron Dosimetry, ASTM STP 341 (1963) 162.
[23] K.L. Murty, E.O. Hall, Dynamic stain aging and neutron irradiation in mild steel, Irradiation Effects on the Microstructure and Properties of Metals, American Society for Testing and Materials STP 611, 1976, pp. 53–71.
[24] K.L. Murty, S.T. Mahmood, Serrated flow in irradiated and partially denitrided mild steel, Proceedings of the 14th ASTM Symposium on Effects of Radiation on Materials, ASTM STP 1046, 1990, pp. 422–430.
[25] K.L. Murty, Mater. Sci. Eng. 59 (1983) 207.
[26] J.E. McLennan, E.O. Hall, J. Aust. Inst. Met. 8 (1963) 191.
[27] K.L. Murty, Nucl. Technol. 67 (1984) 124.
[28] Y.H. Jung, K.R. Narendrnath, P.S. Godavarti, K.L. Murty, A personal computer based system to evaluate J-integral by a single specimen unloading compliance method – Part 1: Methodology, J. Eng. Frac. Mech. 29 (1) (1988) 1; K. Narendrnath, H. Margolin, Y.H. Jung, P.S. Godavarti, K.L. Murty, A personal computer based system to evaluate J-integral by a single specimen unloading compliance method – Part II: Results on A533B class I steel and carona-5, J. Eng. Frac. Mech. 30 (3) (1988) 349.
[29] K.L. Murty, J. Met. 0 (1985) 34.
[30] M. Srinivas, G. Malakondaiah, R.W. Armstrong, P. Rama Rao, Acta Metall. 39 (1991) 807.
[31] G.T. Hahn, A.R. Rosenfield, Application Related Phenomena in Titanium Alloys, ASTM STP 432, 1968, p. 5.